Biomass Conversion and Biorefinery (2021) 11:2347–2358
https://doi.org/10.1007/s13399-019-00508-z

ORIGINAL ARTICLE

Lignin from second-generation biorefinery for pressure-sensitive adhesive tapes

Xihua Hu[1] · Joana Gil-Chavez[1] · Aleksa Hadzi-Ristic[1,2] · Christian Kreft[2] · Cai Rong Lim[2] · Carsten Zetzl[1] · Irina Smirnova[1]

Received: 3 April 2019 / Revised: 29 July 2019 / Accepted: 26 August 2019 / Published online: 31 August 2019
© Springer-Verlag GmbH Germany, part of Springer Nature 2019

Abstract

In this work, the potential of lignin as a filler additive and anti-aging agent in a pressure-sensitive adhesive (PSA) based on natural rubber (NR) was investigated. Herein, different approaches to incorporate lignin into NR matrix by adaptation of a two-step compounding process were evaluated. At first, a twin-screw extruder (TSE) was utilized to prepare pre-formulations followed by the secondary finalization of adhesive mass inside a planetary roll extruder (PRE). For the industrial production of PSAs, the adhesive mass is required to have well-distributed additive materials and adequate adhesion, cohesion, and longevity. The impact of the added lignin was evaluated concerning optical appearance, compatibility between lignin and rubber/resin, adhesion performance, shear strength, thermal stability, antioxidant capability, dynamic-mechanical behavior, aging behavior at elevated temperature and under UV exposure, and filler morphology. It was found that the PSAs including aquasolv (AS) lignin after the spray-drying post-treatment exhibited excellent thermal, mechanical, and antioxidative properties. Thus, it was shown that the sustainably producible lignin can be utilized both as filler and antioxidant in natural rubber-based pressure-sensitive adhesive masses with comparable performance properties as commercially available products.

Keywords Lignin valorization · Press-sensitive adhesives · Liquid hot water · Biorefinery lignin · Particle formulation

1 Introduction

Lignin is the main renewable source of aromatic compounds existing on Earth, and it has been recognized for its potential use in polymer science and as a building block for the sustainable production of chemicals [18]. Due to its aromatic structure and diverse functional groups, the lignin molecule offers numerous options for utilization in product formulation and compounding with other polymers. Nevertheless, its use represents a challenge, since the chemical structure and by extension, its physicochemical properties depend on different factors. Solvents and additives used during the isolation process, operational conditions of the processing steps [6, 7, 20, 39], plant origin, and composition of the plant material, as well as environmental factors affecting the growth of the biomass have an impact on the structural functionalities [3, 34].

For decades, lignin has been produced as a side stream of the pulp and paper biorefineries, where cellulose is the component of major interest. However, in order to fully exploit the biomass potential, current biorefining technologies have emerged aiming at the separation and valorization of the three main biomass components: lignin, cellulose, and hemicellulose. Within this concept, lignin is no longer considered a residue but a source of potential added value [18, 23]. Technologies such as organosolv and hydrothermal processing appear to be promising for the production of high-value lignin as it can be produced sulfur-free and/or solvent-free and sustainably, as they are based on residual biomass. By either using water as solvent or combining the organic solvent recycling process with lignin recovery and particle formulation, the lignin production can be considered to be more environmentally friendly than conventional pulping processes [13, 19, 30].

During hydrothermal pretreatment, a compressed liquid (water) passes through the biomass for 10 to 40 min [8] at pressures from 30 to 50 bar and temperatures varying from 180 to 230 °C [1, 42]. Almost all the hemicellulose is removed

✉ Xihua Hu
xihua.hu@tuhh.de

[1] Institute of Thermal Separation Processes, Hamburg University of Technology, Eissendorfer Strasse 38, 21073 Hamburg, Germany

[2] Rubber Technology and Renewable Materials, tesa SE, Hugo-Kirchberg-Strasse 1, 22848 Norderstedt, Germany

in the first step, while most of the lignin remains in the solid residue linked to cellulose [21]. The pretreated material is subsequently subjected to enzymatic hydrolysis for the cleavage of cellulose into simple sugars, and lignin is lastly separated from the sugar solution. In previous works of our group, a hydrothermal pretreatment process in a fixed bed reactor was developed and implemented in a 40-L pilot plant scale, which allowed the production of so-called aquasolv (AS) lignin. Final composition of 74.6 wt% lignin and 25.4 wt% carbohydrates could be achieved using rye straw as substrate with prior hydrothermal treatment and subsequent enzymatic hydrolysis [23, 28].

Lignin finds its application in biocomposites and packaging, and can be potentially used in adhesive masses, where it could replace parts of adhesive formulations [10]. Due to the phenolic functionality present in lignin, the molecule presents antioxidant capacity and can protect other materials in formulations from being oxidized, thus providing applicability as filler additive as well as a functional compound [9, 35, 40].

The functionality of the aquasolv lignin was proven for the production of aerogels [24] and has shown potential, due to the sustainability of the material across all its processing chain. AS lignin is also a promising candidate for use in polymer and material science, not only because of its "clean nature" but also due to its competitive costs in comparison with lignin obtained in other biorefining processes [29], giving the end products not only ecological but also economical advantage.

Generally, adhesives are classified by their ability to create a bond between different bodies by joining their surfaces either temporarily or permanently. Lignins have recently been applied as adhesive substitutes for wood fiber boards either combined with other biopolymers, such as chitosan [16], or as sole bio-derived constituent [33] making use of the intrinsic compatibility of the lignin/biopolymers and the wood fibers. In phenol-formaldehyde-based (PF) adhesives, different research groups were able to substitute the phenol content of the PF adhesives up to 100% while maintaining comparable performances to commercially available PF resins [17, 41].

Pressure-sensitive adhesives (PSAs) belong to the subclass of non-structural adhesives, which are used to bond materials through adhesion and cohesion. By definition, only light pressure is needed for the adhesion, which does not require any form of activation, such as solvents, heat, or radiation [5, 25]. The application of organosolv lignin in PSAs was recently performed in its native state by blending with a polyether. Results from Sivasankarapillai et al. suggest an interaction of the lignin and the superplasticizers, which improved the overall performance [31]. Wang et al. performed a multi-step synthesis using depolymerized, methanol extracted poplar wood lignin, which resulted in a triblock polymer exhibiting comparable performance to commercial PSAs [38].

In its early stages, PSAs were mainly fabricated from biomass in the form of natural resins and natural rubber [22, 26]. The latter still constitutes 45% of PSA raw materials used in industry because of its availability, cost, and compatibility with different tackifiers and/or plasticizers, which allows the adjustment of the desired adhesion/cohesion balance [2]. However, the isoprene subunits of natural rubber negatively affect the shelf life of the final product, this being a critical factor for material/product performance. In this regard, lignin can be used in NR-based PSAs adding antioxidant properties in addition to its function as filling additive.

The application of PSA in the form of adhesive tapes require an optically homogeneous coating, specific adhesion and cohesion properties, and acceptable shelf life, properties dependent on the distribution of all components. For the distribution of the particulate lignin inside the PSA formulation, small initial particle sizes are advantageous and can be produced and tailored via technologies such as milling and spray-drying. However, small particulate lignin has been shown to exhibit dust explosion potential at particle sizes between 18 and 63 μm according to GESTIS database [14, 15], which would require an appropriate explosion-protected production line. A separate pre-formulation step with another PSA component could limit the additional equipment expenditure by limiting the processing of pre-formulations to isolated facilities away from main production lines, where safety protocols can be implemented more easily. Additionally, two-step compounding could improve the distribution of all components in the final PSA formulation. In this work, different aspects of incorporating lignin obtained via hydrothermal treatment (2nd Generation Biorefinery) into NR-based PSAs, as well as the effect of the lignin particle properties on the performance of the produced materials, were examined. Unlike previous works, lignins are used as received without further modification steps, while the resulting formulations were also subjected to aging tests in order to demonstrate the multi-purpose applicability of the AS lignin.

2 Experimental

2.1 Lignin production

AS lignin was produced in the biorefinery group of the Institute of Thermal Separation Processes at Hamburg University of Technology. The material was obtained from wheat straw as described somewhere else [27]. Briefly, wheat straw was fractionated using the Liquid Hot Water (LHW) pretreatment at 50 bar and 200 °C for 30 min followed by enzymatic hydrolysis (72 h, 50 °C, CTec2 Novozymes). Water-insoluble lignin solids were separated afterwards via decanting and dried as described in Sect. 2.2).

2.2 Particle formation

2.2.1 Spray-dried lignin

Lignin powders were produced in a Niro Mobile Minor laboratory scale spray dryer with co-current flow and two-fluid nozzle with an orifice diameter of 1.5 mm. Ten wt% of AS lignin suspension was fed into the drying chamber through a peristaltic pump with a feeding rate of 65 ml/min. Inlet and outlet temperatures were 172 °C and 110 °C, respectively, and the atomization pressure was at 1.8 bar. The AS lignin powder was collected after the cyclone, and the powder was stored for further experiments and characterization.

2.2.2 Fine milled lignin

Prior to fine milling, the particle size of oven-dried lignin (48 h, 80 °C) was reduced to $D_p < 0.7$–1 mm by a jaw crusher (FRITSCH, Pulverisette 1) and a cross beater mill (FRITSCH, Pulverisette 16) at room temperature. After that, lignin was milled in a planetary ball mill: 5 mm ZrO2 balls were used at 40% filling degree (728 g). In each milling experiment, 90 g lignin was used and the powder+ ball charge was placed in a 500-ml steel beaker. The rotational speed was fixed to 250 min^{-1}, and the milling time was 20 min.

2.3 Particle size determination

The particle size distribution and mean particle size analysis of the powders were performed on laser diffraction particle size analyzer equipped with a Tornado dry powder system (LS 13320, Beckman Coulter, USA). The Fraunhofer theory was used for the determination of the diameters and size distributions.

2.4 Lignin analysis

Determination of lignin and residual sugar content was conducted with a modified method from TAPPI [32]. Two hundred milligrams of ground particulate material was subjected to 2 mL of 72 wt% sulfuric acid at 30 °C for 1 h. Pre-hydrolysis was halted with the addition of 56 mL deionized water. Second hydrolysis was conducted at 120 °C and 2.2 bar for 40 min and was diluted after treatment with 100 mL deionized water. Hydrolysate was analyzed for the sugar monomers using anion exchange chromatography (HPAEC) with borate buffer as mobile phase and a fluorescence detector. Hydrolysate residues were washed and dried until constant mass with subsequent ash content determination via heating until 550 °C. Non-ash residue was considered as lignin content.

2.5 Pre-compounding in TSE

Pre-formulations of lignin/natural rubber and lignin/tackifier resin were produced inside a twin-screw extruder (TSE), Leistritz ZSE 27 MAXX, with a L/D ratio of 48. Throughput of total material was fixed at 3 kg/h with varying mass ratios of lignin to polymer (10–40 wt% lignin), barrel temperatures (120–160 °C), and screw speeds (100–300 rpm). Samples were produced without an extrusion die and collected after steady state was reached.

2.6 PSA formulation

Final formulation of PSA was conducted inside a planetary roll extruder (PRE) manufactured by ENTEX Rust & Mitschke GmbH. Compounding conditions were fixed at 120 °C barrel/extruder die temperature, 50 rpm screw speed, and 10 kg/h throughput. Pre-formulated material was introduced with NR with the subsequent optional addition of molten tackifier resin and particulate material as final component. Content of components in final PSA formulation was fixed at 42% of NR, 41% of hydrocarbon tackifier resin, and 17% of either lignin or $CaCO_3$/TiO_2/anti-oxidant premixture.

2.7 Distribution in pre-mixes

ASLM and ASLSD particle size within the tack resin matrix were studied via solvent casting in n-heptane and light microscope image analysis with regard to different TSE process parameters. To investigate lignin PSD and agglomeration behavior, images were taken and processed by Fiji software and BioVoxxel Toolbox plugin. Ideal sphere diameter for each particle was calculated from the particle area to obtain number distribution of lignin particles within the resin matrix.

2.8 Rheological data of pre-formulations

Rheological analysis was performed to determine complex viscosity of pre-formulations with different lignin contents by means of an RPA 2000 from Alpha Technologies. Frequency sweep was conducted with oscillation frequencies from 0.1 to 1000 rad/s and an oscillation amplitude of 5% strain at 120 °C for a sample volume of approximately 4.5 cm^3 and an amount of 5 g/sample.

2.9 Thermal properties (DSC, TMDSC, TGA)

DSC measurements were conducted with DSC 204 F1 Phoenix (Netzsch). For T_G measurements, samples were analyzed from − 140–200 °C at a heating rate of 10 K/min and nitrogen flow rate of 20 mL/min. Glass transition temperatures were reported as the transition midpoint of the heat capacity change by taking the data obtained from the second heating cycle.

Oxidation induction time (OIT) analysis was performed using the same apparatus to quantify the thermal stabilization provided by anti-oxidative agents. From each formulation, a sample of 5 mg was placed in a non-sealed aluminum pan. Samples were heated to 170 °C at 15 K/min under nitrogen atmosphere; it was subsequently kept at 170 °C for 2 min to equilibrate isothermal conditions and then subjected to an oxygen atmosphere. From this moment, the time until occurrence of the exothermic peak was recorded as the OIT.

Temperature modulated DSC analysis was conducted with a DSC 3 from Mettler Toledo to detect reversible and non-reversible heat flows in order to discern glass transition temperature from other thermal effects of different types of lignin. Samples of approximately 25 mg were placed in aluminum crucibles and tested from 30 to 230 °C at a heating rate of 1 K/min and nitrogen flow of 30 mL/min.

TGA analyses were carried out on a TG 209 F1 Libran (Netzsch) with samples of around 15 mg placed in alumina crucibles. The mass of each sample and empty alumina crucible, which served as a reference, was recorded. The tests were performed under an air atmosphere with the airflow rate of 20 mL/min and a temperature range from 25 to 900 °C at a heating rate of 20 K/min.

2.10 Determination of –OH content via titration

The –OH content of fine-milled and spray-dried AS lignins was determined via titration of prior esterified samples against a methanolic potassium hydroxide solution. Briefly, 1 g of lignin sample was suspended in 15 mL *N*-methyl-2-pyrrolidone containing 1 wt% of 4-(dimethylamino) pyridine. Five milliliters of acetic anhydride was added, and samples were stirred for 1 h. Esterification was stopped by adding 2 mL of water to hydrolyze residual anhydride. Samples and blanks were titrated against a 0.5 M KOH solution.

2.11 PSA testing methods

Peel adhesion (PA) testing of finalized PSA tapes was performed to determine adhesive strength. Unless otherwise indicated, the measurements were carried out at 23 ± 10 °C and 50 ± 5% relative humidity. Steel plates and polyethylene (PE) plates were used as a substrate for PA measurements. The cured adhesive sheet under investigation was cut to a width of 20 mm and to a length of approximately 250 mm. Immediately thereafter, the strip was pressed onto the selected substrate using a 4-kg steel roller, with speed of 10 m/min. Then, the adhesive strip is peeled from the substrate at an angle of 180° using a tensile testing machine (Zwick/Roell), and the required force was recorded. The PA value (in N/cm) is obtained as the average from three measurements.

Shear strength was measured for determination of cohesive strength. PSA strip of 10 mm width was attached to a steel test plate by rolling with 2 kg three times back and forth (10 m/min). Reinforcement material was applied on the upper part of the strip, and a clamp was equipped on the lower part of the sample. The specimen was subjected to shear stress by 300-g weight for 15 min at 40 °C. Afterward, the weight is automatically taken off and the sample is allowed to relax (slip back) for another 15 min. The result is the displacement after shearing and relaxation at a constant temperature. The test was conducted in duplicates. A commercially available PSA containing the $CaCO_3/TiO_2$/antioxidant mixture instead of lignin, referred to as standard formulation (SF), was taken as a benchmark for comparison with lignin-containing samples for both peel adhesion and shear strength testing.

2.12 Aging methods

Two accelerated aging methods were applied to test the longevity of PSAs. Elevated temperature was applied to PSA tapes inside an air-circulating oven for 14, 28, and 42 days at 60 °C and 50% relative air humidity. Cohesion and adhesion tests were conducted via microshear and PA according to previously described methods, respectively.

UV-induced aging was conducted with cut PSA samples (20 cm × 25 cm) adhered to a quartz glass plate with a thickness of 4 mm adhered by using a 2-kg roller (10 m/min) five times. Glass plates were previously cleaned with acetone. The specimens were stored with the glass side upward in a UV weathering chamber with a xenon lamp, SunTest XXL+ (Atlas), under an irradiance of 60 W/m^2, temperature of 38 °C, and relative humidity of 50%. Initially, every 2 h during the first 24 h period, one new strip per sample was taken from the chamber and, after conditioning to room temperature for 1 h, peeled from the glass surface. The standard protocol for PA measurements was followed. On the following days, one new strip per PSA sample was taken and bond strength was determined. During the procedure, optical quality of adhesive residues after peel was recorded.

3 Results and discussion

3.1 Particulate material

3.1.1 Hydrolytic lignin properties

The Klason lignin content is one of the most important criteria in lignins and evaluates the effectiveness of the biorefining processes for the separation of lignin from their original matrices; in the case of the AS lignins, Klason content gives also the performance of the enzymatic hydrolysis and separation of cellulose [24]. The AS lignin utilized in this study had Klason lignin of 85(± 2) wt%, 13.5(± 1.3) wt% polysaccharides, 1.4(± 0.2) wt% acid-soluble lignin, and small amount of

inorganics typical for wheat straw lignins. The remaining amount of polysaccharides is covalently linked to the lignin and/or can be entrapped in its branched structure, hindering cellulases from accessing them within enzymatic hydrolysis.

3.1.2 Lignin particle formulation

AS lignin fine powders used in this study were obtained through planetary ball milling (ASLM) and spray drying (ASLSD), and processing parameters were previously adjusted for producing AS lignin particles with a size of $D_{50} <$ 30 μm, this latter, aiming a homogeneous distribution within the adhesive formulation. ASLM was obtained in sizes of $D_{10} = 1.37$ μm and $D_{50} = 6.03$ μm (Fig. 1a), while ASLSD size was of $D_{10} = 3.7$ μm and $D_{50} = 13.8$ μm (Fig. 1b).

Scanning electron microscopy (SEM) images of ASLM and ASLSD were taken for characterization of the particle's morphology. As observed in Fig. 1a, particles of ASLSD have a spherical form, and such morphology is typically found in spray-dried powders. In this process, the feed (i.e., lignin suspension) is atomized through a nozzle into the drying chamber in a sheet-like flow, however; due to the atomization pressure, this gets broken down to smaller ligaments and further into fine droplets [36, 37]. During drying, the viscosity of the droplet increases, the solvent content decreases, and the solidification of the droplet occurs. Thus, at the end of the process,

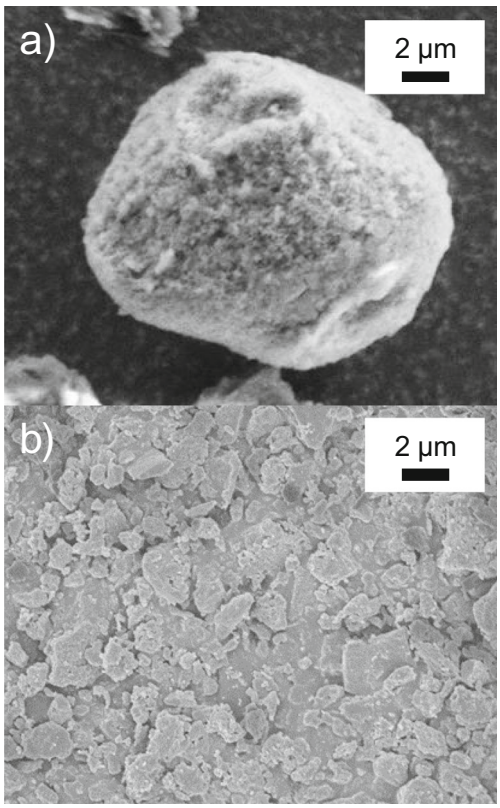

Fig. 1 SEM images of AS lignin powders obtained via **a**) spray drying and **b**) planetary ball mill

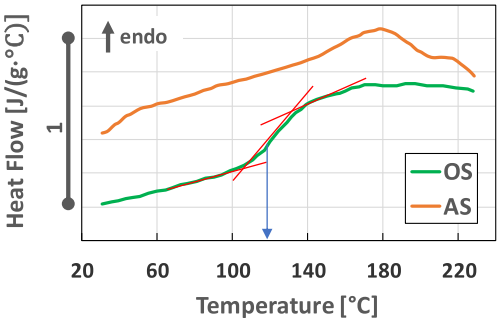

Fig. 2 Thermogram of reversing heat flow from temperature modulated DSC of organosolv (OS) lignin from beech wood and spray-dried aquasolv (AS) lignin from wheat straw

the dried particle will have the form of the spherical droplet as it is assumed that the particle dries at a constant evaporation rate and the droplet diameter decreases linearly.

In Fig. 1b, it can be seen that ASLM presented an irregular particle morphology with a flattened-like shape. During ball milling, different stresses (compression, attrition, shear, and impact) in the particles being ground can be present depending on the nature of the initial material and the particle size of the milling balls as well as the ball charge [4]. When the milling balls collide, a small portion of the particles is trapped (compressed) between them resulting in flattened structures [11]. Increasing ball milling times (2–4 h) results in the formation of overlapped flattened layers (sandwich microstructure), nevertheless; the 20-min milling time used in this work leads to elongation (particle flattening) followed by fracturing/fragmentation (size reduction) of the materials, thus resulting in very fine powders in short milling time.

3.1.3 Thermal properties

Due to the residual sugar contents of the lignin, the processing temperature range has to be taken into account for the incorporation, in order to either prevent unwanted condensation reactions with the polymer matrix or evaporation of degradation products. Different thermal analyses were applied to further specify processing conditions for the lignin/resin compounds.

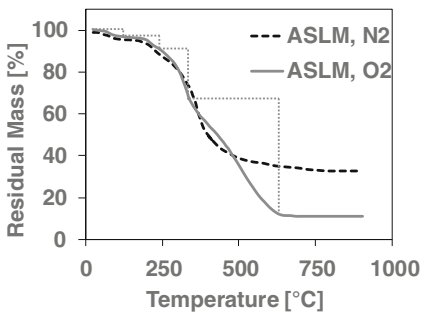

Fig. 3 TGA results of ASLM under nitrogen and normal atmosphere; dotted lined indicates significant mass loss steps

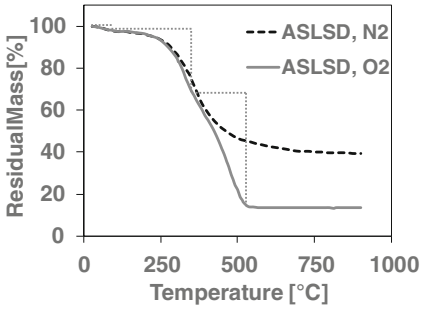

Fig. 4 TGA results of ASLSD under nitrogen and normal atmosphere; dotted lined indicates significant mass loss steps

Temperature modulated DSC (TMDSC) of particulate lignin was conducted, as initial DSC analysis did not reveal glass transition behavior of the aquasolv lignin. With the TMDSC, the reversing heat flow could be discerned from the overlaying effects, such as evaporation and heat effects from reactions. Figure 2 suggests a significant difference between the aquasolv lignin and other established technical and non-technical lignins. Contrary to other lignin isolation methods, the obtained aquasolv lignin does not show a glass transition. This could be attributed to the sequence of fractionation steps and the treatment parameters during lignin isolation. Organosolv lignin, for instance, shows a transition range between 100 and 140 °C, which agrees well with literature [12], whereas aquasolv lignin only shows a linear decrease in heat flow within that range.

TGA analysis was performed at a heating rate of 20 K/min. Figures 3 and 4 show the temperature-dependent mass loss of ASLM and ASLSD under nitrogen and normal atmosphere, respectively. Analysis of the mass loss under normal atmosphere suggests an additional 5% mass loss between 120 and 240 °C for the milled lignin, whereas this loss step is not observed for the spray-dried lignin. It is hypothesized that due to higher temperatures during spray drying, volatile compounds are removed from the lignin particles, which otherwise would adhere to the surface of the particles as during oven drying prior to milling. This temperature range could correspond with residual sugars, sugar degradation products from pre-treatment, or volatile phenolic compounds from the native lignin.

Table 1 Hydroxyl content of utilized lignins determined by titration against potassium hydroxide after esterification (standard deviation with $N = 2$)

Sample	OH-number (mgKOH/g)
ASLSD	140.98 ± 3.13
ASLM	140.25 ± 2.96

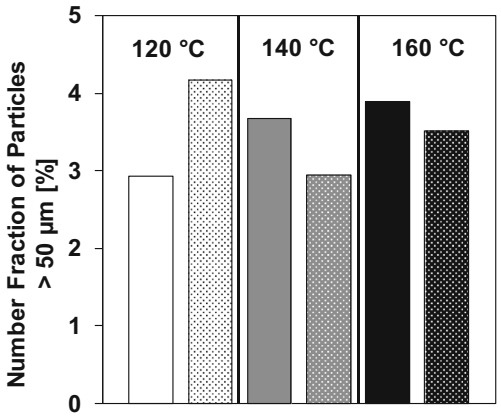

Fig. 5 Number fraction of lignin particles inside tackifier resin (33/67 wt%) larger than 50 µm for ASLM (filled) and ASLSD (shaded) at different compounding temperatures; at least 5000 particles per sample analyzed with two samples per data point

3.1.4 Hydroxyl content

The –OH content of fine-milled and spray-dried lignins was determined in order to assess the influence of their chemical functionality on the lignin-polymer interactions with the adhesive matrix. Results from Table 1 indicate that both aquasolv lignins exhibited comparable hydroxyl functionality despite their different formulation processes. Residual adhered compounds as suggested by TGA results did not contribute towards the –OH content. In terms of lignin polymer interaction, both AS lignin types should exhibit similar behavior. Thus, discrepancies in resulting adhesive compound properties can assumedly be related to the species of –OH, which was not determined using this titration method and/or the compounds retained within the milled lignin fraction.

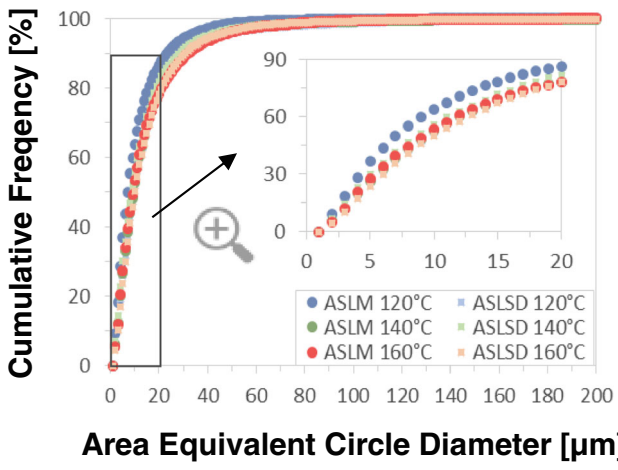

Fig. 6 Cumulative number frequency of lignin particles sizes found in tackifier resin matrix for ASLM and ASLSD at different compounding temperatures

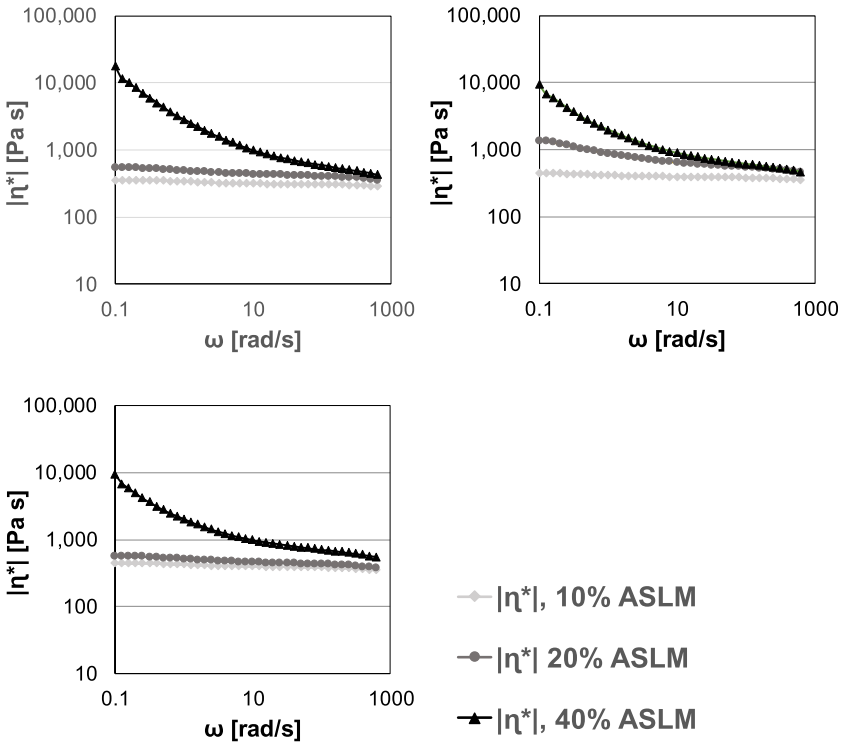

Fig. 7 Frequency sweep of lignin/tackifier resin compounds with different ASLM contents

3.2 Pre-compounds

3.2.1 Compounding

Pre-compounding of particulate lignin with tackifier resin was conducted in order to investigate a two-step production process of lignin-containing PSA tapes. Due to the flammability of lignin particles and the accompanying risk of dust explosion, a secluded pre-compounding site with required safety equipment and protocols would be more feasible than to include safety precautions on the main production site. In addition, the first compounding step would act as a pre-distribution of the particulate material into the polymer matrix, allowing for better dispersion and distribution in the secondary compounding step.

Microscopy analysis of the pre-compounds revealed no significant influences of different compounding

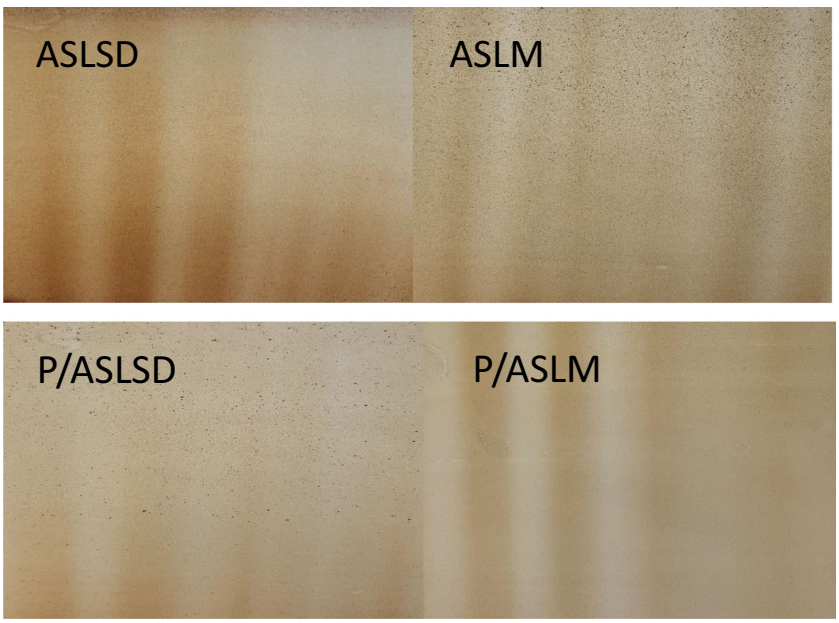

Fig. 8 Finalized and coated PSA with 50 g/m^2 thickness with particulate lignin and pre-compounded lignin/tackifier resin

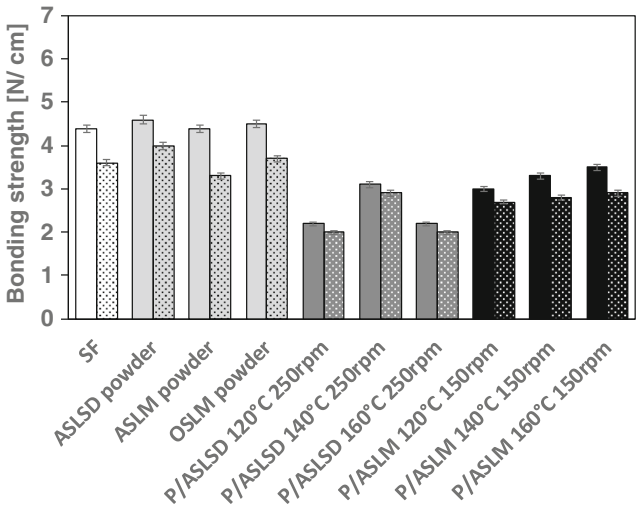

Fig. 9 Bonding strength from peel adhesion tests on steel (filled) and polyethylene (shaded) for standard formulation (SF), PSAs with lignin added in powder form or as pre-formulations

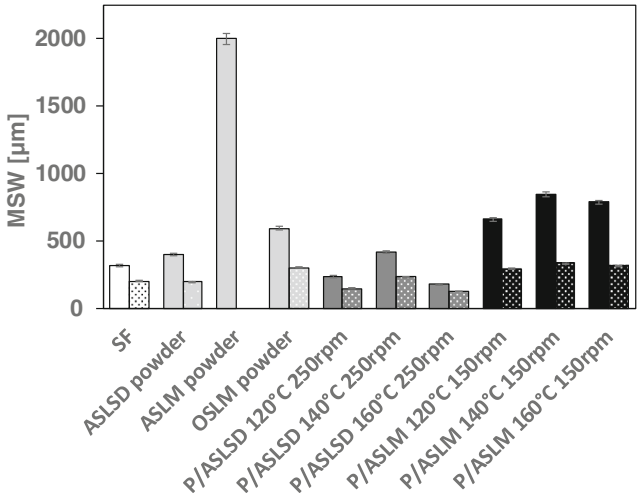

Fig. 11 Micro shear distances (MSW) from shear strength tests at 3 N and 40 °C after 15 min (filled) and displacement after relaxation (shaded) of standard formulation (SF), PSAs with lignin added in powder form or as pre-formulations after 4 weeks storage at 60 °C

parameters within the investigated ranges with regard to the number fraction of particles, which is larger than 50 µm (Fig. 5). This specific particle size has been chosen, due to the coating thickness of the finalized PSA tapes, which therefore might cause coating errors in the final production of PSA tapes. The cumulative number frequency shows marginally higher amounts of smaller particles with ASLM at 120 °C (Fig. 6). However, this did not significantly affect the number of particles larger than 50 µm compared to the other parameter sets. The negligible influence of compounding parameter and type of lignin for the pre-compounds are likely to be explained by the rheological properties.

3.2.2 Rheological analysis

The rheological analysis of the pre-compounds reveals almost identical progression during the frequency sweep with the exception at 140 °C (Fig. 7). As the applied screw speed during compounding lies between 100 and 300 rpm, which would correspond approximately to 10 to 30 rad/s, the actual differences in viscosities would be within an order of magnitude and therefore not having a high impact during the compounding process for particle break-up to occur. The lignin contents contribute slightly to higher viscosities above 20 wt%, which again would result in a marginal increase in viscosity, considering the shear rate ranges.

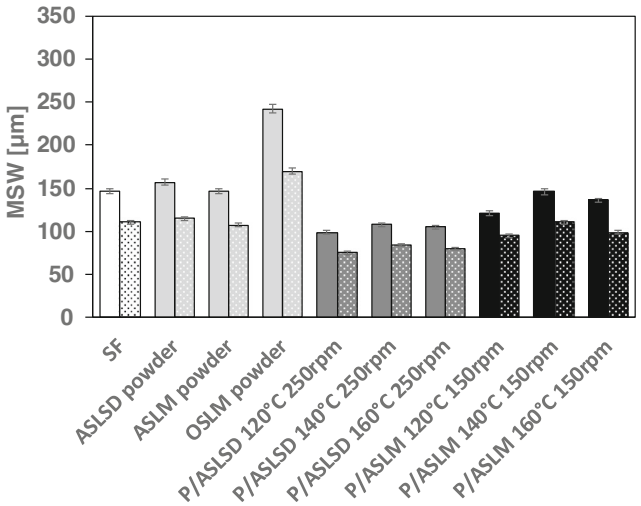

Fig. 10 Micro shear distances (MSW) from shear strength tests at 3 N and 40 °C after 15 min (filled) and displacement after relaxation (shaded) of standard formulation (SF), PSAs with lignin added in powder form or as pre-formulations

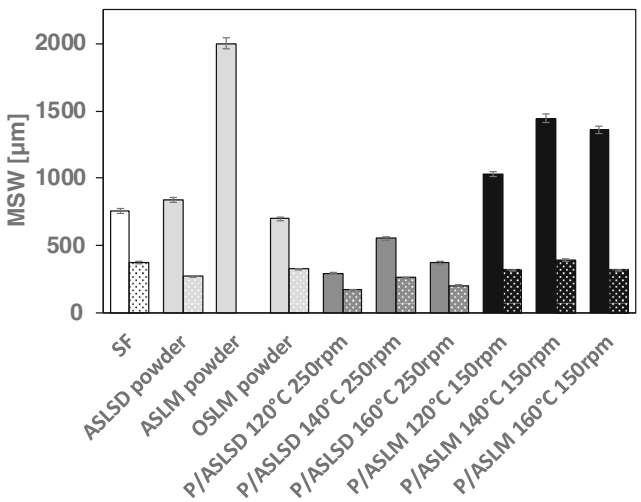

Fig. 12 Micro shear distances (MSW) from shear strength tests at 3 N and 40 °C after 15 min (filled) and displacement after relaxation (shaded) of standard formulation (SF), PSAs with lignin added in powder form or as pre-formulations after 6 weeks storage at 60 °C

3.3 Pressure-sensitive adhesive formulations

3.3.1 Appearance

Coated PSA formulation containing lignin is shown in Fig. 8. General appearances of the coated tapes show no coating failures caused by particle agglomerates, and the overall distribution of the particles can be classified as uniform. However, visible particles are still to be observed for PSAs compounded with the powder lignins and the PSA with pre-compounds of tackifier resin and ASLSD. In terms of numbers from image analysis, these amount to approximately 2200, 2700, 1650, and 60 particles per square meter for ASLSD, ASLM, P/ASLSD, and P/ASLM, respectively.

These findings suggest that although the pre-compounding shows similar particle size distributions, the addition of pre-compounded material and the finalization of PSA formulation depend on the lignin particle type. In the case of ASLM, particle agglomerates were successfully broken up during compounding in the PRE, whereas ASLSD particles seemingly remained as particle clusters inside the pre-compounds. This behavior could be attributed to the morphology of the particles. The sphericity of the spray-dried particles impedes particle breakup, whereas the flaky structure of the milled lignin allowed a better diminution and thereby local dispersion. Due to the significantly lower viscosity of the resin compared to the PSA mass, the difference in morphology did not have as high an impact as with the finalized PSA. This would explain the obtained results from both microscopy and image analyses.

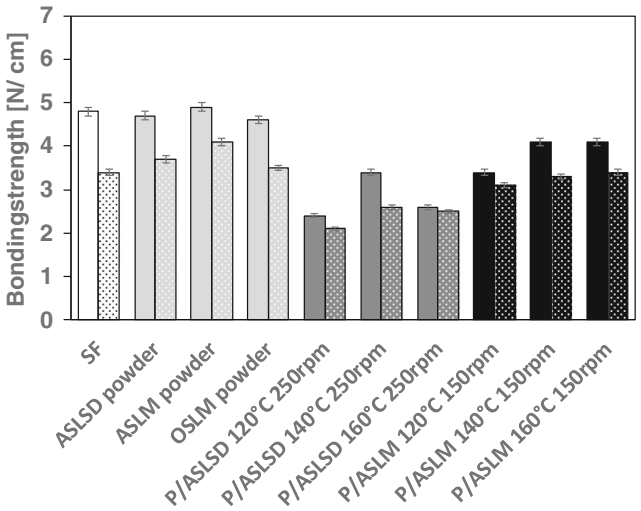

Fig. 13 Bonding strength from peel adhesion tests on steel (filled) and polyethylene (shaded) for standard formulation (SF), PSAs with lignin added in powder form or as pre-formulations after 4-week storage at 60 °C

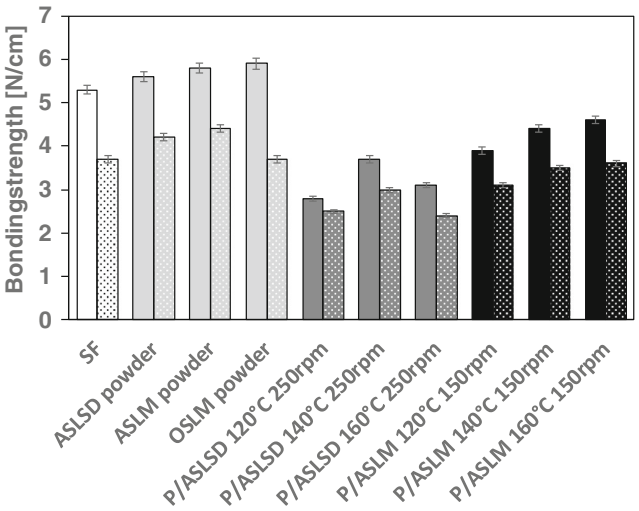

Fig. 14 Bonding strength from peel adhesion tests on steel (filled) and polyethylene (shaded) for standard formulation (SF), PSAs with lignin added in powder form or as pre-formulations after 6-week storage at 60 °C in comparison with standard formulation (SF)

3.3.2 PSA performance: standard vs. lignin

Performance of the coated PSA formulation was tested with regard to their adhesion on surfaces and cohesion within the adhesive mass with the peel adhesion test and shear strength test, respectively. For peel adhesion, both steel and polyethylene as polar and nonpolar surfaces were tested. Shear strength was expressed as micro shear distance (MSW). After 15 min of initial loading, the displacement after relaxation is compared to the initial displacement. Lower values for initial displacement and total displacement after relaxation represent higher cohesive behavior of the adhesive. Figures 9 and 10 indicate that PSAs with directly incorporated aquasolv lignins have similar performance properties as the standard formulation. PSAs with ASLSD pre-compounds show lower adhesion, while also possessing higher cohesion. This dependency is to be expected, as higher cohesive strength is accompanied by a lower capability to wet the surface, thus showing a decreased bonding strength. P/ASLM samples have comparatively higher bond strength than P/ASLSD, while also showing lower cohesion. Generally, the initial performance of PSAs containing particulate AS lignin (light gray) has

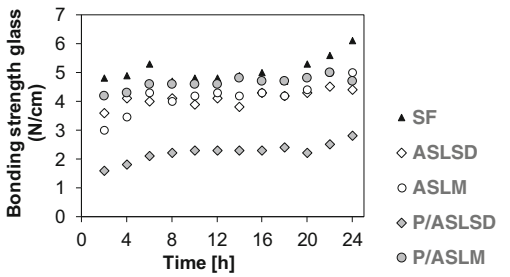

Fig. 15 Bonding strength from peel adhesion tests after UV aging for standard formulation (SF) and selected samples over initial 24 h

Fig. 16 PSA tapes subjected to UV irradiation and subsequent peel test after 24 h (left) and 8 days (right) in the following order: SF, ASLM, ASLSD, P/ASLSD, P/ASLM

properties closest to the standard formulation, although the appearance of the tape showed local particle aggregations. Meanwhile, pre-compounded materials with P/ASLM had the best appearances.

3.3.3 Aging tests

The longevity of NR-based PSA is limited by the chemical structure of the natural rubber. Due to the double bonds of the isoprene units, the polymer matrix is prone to oxidation. Shear strength measurements were conducted after storage of the PSAs at elevated temperature of 60 °C. Storage time of 6 weeks at these conditions correspond to 24 months at room condition. Figures 11 and 12 show micro shear distances after 4 weeks and 6 weeks of accelerated aging. The most notable sample is the PSA with ASLM powder, which failed the shear strength test after initial loading force. Samples with P/ASLM showed an increase in MSW indicating gradual deterioration of the rubber matrix over time, although no trend with regard to pre-compounding parameters could be observed. This implies that ASLM has a lower anti-oxidative capacity, which is needed to protect the rubber matrix from oxidation. Analyses of the thermal properties of the different AS lignin types suggest that adhered volatile compounds and/or residual sugars are present with the oven-dried, milled lignin. This might cause inaccessibility of the phenolic groups within the lignin, which are attributed to the radical scavenging properties. Cohesion behavior was mostly conserved in the P/ASLSD samples, which slightly surpass samples with particulate ASLSD in terms of cohesive strength. Samples containing either OS or ASLSD lignins were able to protect the rubber matrix, thereby successfully substituting the commercially available anti-oxidants within the standard formulation, which makes them viable for application as both filler additive and aging protectant.

Adhesion behavior of aged samples showed a slight increase in all cases (Figs. 13 and 14), which is to be expected, due to the decrease in the cohesion of the adhesive and therefore an improvement of overall surface wetting. It is interesting to note that the adhesion increase is more prominent on steel surfaces in the majority of cases. This is presumably caused by oxidized carbon double bonds of the natural rubber matrix.

PSAs were also subjected to UV aging in order to evaluate protection capabilities from other oxidizing sources. Twenty-four hours of irradiation at 60 W/m^2 corresponds to 30 days with 10 h of sunlight per day. Adhesion properties of the initial 24 h are presented in Fig. 15. Gradual increase of bonding strength was observed for all samples accompanied by

Table 2 Thermal properties of selected samples with their respective mass loss steps (ML1–3), residual mass, temperatures at the mass loss of 10 (T, 10%) and 50% (T, 50%), and glass transition temperature (T, G)

Sample	Residue at 900 °C (wt%)	ML, 1 (wt%)	ML, 2 (wt%)	ML, 3 (wt%)	T, 10% (°C)	T, 50% (°C)	T, G (°C)
SF	11.0	61.2	18.8	9.0	348	398	− 51
ASLSD	3.8	62.1	23.5	10.4	329	388	− 50
ASLM	8.1	63.8	20.9	7.2	339	389	− 51
P/ASLSD 120 °C	4.3	63.2	24.6	7.7	340	389	− 53
P/ASLSD 140 °C	4.4	61.3	26.6	7.6	340	389	− 54
P/ASLSD 160 °C	3.1	60.0	29.4	7.1	338	384	− 53
P/ASLM 120 °C	6.3	60.0	28.2	5.5	340	383	− 54
P/ASLM 140 °C	6.5	59.9	28.1	5.6	342	384	− 50
P/ASLM 160 °C	5.4	61.8	27.8	5.1	342	385	− 54

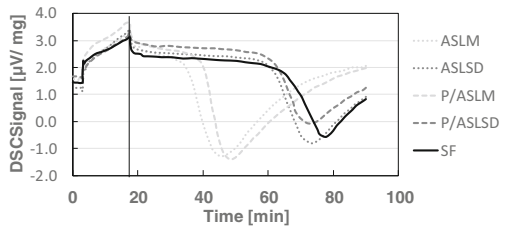

Fig. 17 Oxidation induction time of particulate-milled (ASLM) and spray-dried lignin (ASLSD) as well as PSA formulations of the standard recipe (SF) and respective lignins (P/ASLM and P/ASLSD)

cohesion failure at the tape brims. Nevertheless, the tapes, with the exception of ASLM, were all successfully removable from the glass surface after eight consecutive days of UV radiation (Fig. 16). These results correspond well with the accelerated aging under elevated temperatures and confirm previous findings that downstream processing of the lignin has a major influence on the properties and functionalities within polymeric matrices.

3.3.4 Thermal properties

TGA and DSC analyses were performed with finalized PSA formulations, which are summarized in Table 2. Higher amounts of residues at 900 °C for SF and ASLM-containing PSAs suggest greater fractions of inorganics, whereas overall mass loss progression (ML1–3) only shows negligible differences.

In addition to thermal characterization using TGA and DSC, the oxidation induction time (OIT) was investigated. OIT is an indicator of the thermo-oxidative stability of formulated adhesives. As indicated in Fig. 17, degradation of adhesives is induced after the atmosphere is switched from inert to oxidative. When the capacity of antioxidants is reached, the reaction proceeds at a much faster rate, which manifests in a detectable exothermic heat signal. Thus, a prolonged OIT indicates a higher antioxidant capacity.

Based on the presented results, adhesives containing ASLSD showed a similar antioxidative effect in comparison to the standard formulation containing commercial antioxidants with an OIT at 66 min, whereas samples with milled lignins, whether in particulate or pre-compounded form, show decreased induction times. These results are in accordance with the results of shear strength measurements after accelerated, heat-induced aging, as well as TGA analysis of the particulate lignins. It suggests that the residuals adhered to ASLM during oven drying procedure would cause interference with the antioxidative capabilities of the lignin.

4 Conclusions

AS lignin obtained from biorefinery process was micronized via spray-drying technology and planetary ball milling and were used for adhesive formulation; two different powder sizes, particle size distributions, and morphologies were obtained, and a correlation between these and adhesion strength of adhesive tapes and dispersion in the product was assessed. Overall, ASLSD particles showed a better performance in the product prototype when compared to ASLM. Particle size distribution can be further improved in order to potentiate its applicability and functionality.

During thermal analyses, it was shown that ASLM in both particulate and pre-compounded form had volatile compounds adhered, which resulted in lower aging protective properties. It is hypothesized that the potential cause is the hindered access to phenolic structures of the lignin molecule. Nevertheless, the morphology of the ASLM allowed particle diminution during PRE-compounding of the PSA mass leading to optically homogeneously coated tapes.

PSAs containing ASLSD were found to reach comparable performance of standard, commercially available PSA formulations even though some amounts of particles were still discernable on the adhesive tapes. The pre-compounded material P/ASLSD performed better in the aging tests, while exhibiting lower adhesion strength. However, adjustment of the formulation with an increase of tackifier resin amount could compensate for the lower adhesion. Therefore, we can conclude that spray-dried lignin from second-generation biorefinery is a possible replacement for commercial antioxidant while also serving as filler material for the production of NR-based PSAs, which opens up new application possibilities utilizing both mechanical (filler) and physicochemical properties (antioxidant) of lignin.

Funding information This work was financially supported by the German Federal Ministry of Education and Research (BMBF) in the context of the German project cluster BIOREFINERY2021 (031A233).

References

1. Agbor VB, Cicek N, Sparling R, Berlin A, Levin DBJB (2011) Biomass pretreatment: fundamentals toward application. 29(6): 675–685
2. Benedek I, Feldstein MM (2008) Technology of pressure-sensitive adhesives and products. CRC press
3. Boerjan W, Ralph J, Baucher M (2003) Lignin biosynthesis. Annu Rev Plant Biol 54(1):519–546
4. Canakci A, Erdemir F, Varol T, Patir AJM (2013) Determining the effect of process parameters on particle size in mechanical milling using the Taguchi method: measurement and analysis. 46(9):3532–3540
5. Cantor AS, Menon VPJE o. P. S., & technology (2002) Pressure-sensitive adhesives
6. Chung H, Washburn NR (2016) Extraction and types of lignin. In: Lignin in polymer composites. Elsevier, pp 13–25. https://doi.org/10.1016/B978-0-323-35565-0.00002-3
7. El Hage R, Brosse N, Chrusciel L, Sanchez C, Sannigrahi P, Ragauskas A (2009) Characterization of milled wood lignin and ethanol organosolv lignin from Miscanthus. Polym Degrad Stab

94(10):1632–1638. https://doi.org/10.1016/j.polymdegradstab.2009.07.007
8. Gairola K, Smirnova IJ Bt (2012) Hydrothermal pentose to furfural conversion and simultaneous extraction with SC-CO2–kinetics and application to biomass hydrolysates. 123:592–598
9. García A, Alriols MG, Spigno G, Labidi J (2012) Lignin as natural radical scavenger. Effect of the obtaining and purification processes on the antioxidant behaviour of lignin. Biochem Eng J 67:173–185
10. Ghaffar SH, Fan M (2014) Lignin in straw and its applications as an adhesive. Int J Adhes Adhes 48:92–101. https://doi.org/10.1016/j.ijadhadh.2013.09.001
11. Gorrasi G, Sorrentino AJGC (2015) Mechanical milling as a technology to produce structural and functional bio-nanocomposites. 17(5):2610–2625
12. Hansen B, Kusch P, Schulze M, Kamm B (2016) Qualitative and quantitative analysis of lignin produced from beech wood by different conditions of the organosolv process. J Polym Environ 24(2):85–97. https://doi.org/10.1007/s10924-015-0746-3
13. Ingram T, Wörmeyer K, Lima JCI, Bockemühl V, Antranikian G, Brunner G, Smirnova, I. J. B. t. (2011) Comparison of different pretreatment methods for lignocellulosic materials. Part I: conversion of rye straw to valuable products. 102(8):5221–5228
14. Institut für Arbeitsschutz der Deutschen Gesetzlichen Unfallversicherung. GESTIS-STAUB-EX: Lignin - 1, 2019
15. Institut für Arbeitsschutz der Deutschen Gesetzlichen Unfallversicherung. GESTIS-STAUB-EX: Lignin - 2, 2019
16. Ji X, Guo M (2018) Preparation and properties of a chitosan-lignin wood adhesive. Int J Adhes Adhes 82:8–13. https://doi.org/10.1016/j.ijadhadh.2017.12.005
17. Kalami S, Arefmanesh M, Master E, Nejad M (2017) Replacing 100% of phenol in phenolic adhesive formulations with lignin: ARTICLE. J Appl Polym Sci 134(30):45124. https://doi.org/10.1002/app.45124
18. Laurichesse S, Averous L (2014) Chemical modification of lignins: towards biobased polymers. Prog Polym Sci 39(7):1266–1290
19. Lora J (2008) Industrial commercial lignins: sources, properties and applications. In: Monomers, polymers and composites from renewable resources. Elsevier, pp 225–241
20. Luo H, Abu-Omar MM (2018) Lignin extraction and catalytic upgrading from genetically modified poplar. Green Chem 20(3):745–753. https://doi.org/10.1039/C7GC03417B
21. Mosier N, Wyman C, Dale B, Elander R, Lee Y, Holtzapple M, Ladisch MJ Bt (2005) Features of promising technologies for pretreatment of lignocellulosic biomass. 96(6):673–686
22. Osswald T, Hernández-Ortiz JPJM, Hanser SM (2006) Polymer processing, pp 1–651
23. Perez-Cantu L, Schreiber A, Schütt F, Saake B, Kirsch C, Smirnova I (2013) Comparison of pretreatment methods for rye straw in the second generation biorefinery: effect on cellulose, hemicellulose and lignin recovery. Bioresour Technol 142:428–435
24. Perez-Cantu L, Liebner F, Smirnova IJM, Materials M (2014) Preparation of aerogels from wheat straw lignin by cross-linking with oligo (alkylene glycol)-α, ω-diglycidyl ethers. 195:303–310
25. Pizzi A, Mittal KL (2017) Handbook of adhesive technology. CRC press
26. Rauwendaal C (2014) Polymer extrusion. Carl Hanser Verlag GmbH Co KG
27. Reynolds W, Kirsch C, Smirnova IJCIT (2015) Thermal-enzymatic hydrolysis of wheat straw in a single high pressure fixed bed. 87(10):1305–1312
28. Reynolds W, Baudron V, Kirsch C, Schmidt LM, Singer H, Zenker L, Zetzl C, Smirnova I (2016) Odor-free lignin from lignocellulose by means of high pressure unit operations: process design, assessment and validation. Chem Ing Tech 88(10):1513–1517. https://doi.org/10.1002/cite.201600005
29. Schmidt LM, Martínez VP, Kaltschmitt MJ Bt (2018) Solvent-free lignin recovered by thermal-enzymatic treatment using fixed-bed reactor technology–economic assessment. 268:382–392
30. Schulze P, Seidel-Morgenstern A, Lorenz H, Leschinsky M, Unkelbach G (2016) Advanced process for precipitation of lignin from ethanol organosolv spent liquors. Bioresour Technol 199:128–134. https://doi.org/10.1016/j.biortech.2015.09.040
31. Sivasankarapillai G, Eslami E, Laborie M-PG (2019) Potential of organosolv lignin based materials in pressure sensitive adhesive applications. ACS Sustain Chem Eng 7:12817–12824. https://doi.org/10.1021/acssuschemeng.9b01670
32. Standard, T. J. T.o (2002). Acid-insoluble lignin in wood and pulp
33. Theng D, El Mansouri N-E, Arbat G, Ngo B, Delgado-Aguilar M, Pèlach MÀ, Fullana-i-Palmer P, Mutjé P (2017) Fiberboards made from corn stalk thermomechanical pulp and kraft lignin as a green adhesive. BioResources 12(2). https://doi.org/10.15376/biores.12.2.2379-2393
34. Vanholme R, Demedts B, Morreel K, Ralph J, Boerjan W (2010) Lignin biosynthesis and structure. Plant Physiol 153(3):895–905
35. Vazquez-Olivo G, López-Martínez LX, Contreras-Angulo L, Heredia JB (2017) Antioxidant capacity of lignin and phenolic compounds from corn stover. Waste Biomass Valorization:1–8
36. Vicente J, Pinto J, Menezes J, Gaspar FJ Pt (2013) Fundamental analysis of particle formation in spray drying. 247:1–7
37. Walton DJDT (2000) The morphology of spray-dried particles a qualitative view. 18(9):1943–1986
38. Wang S, Shuai L, Saha B, Vlachos DG, Epps TH (2018) From tree to tape: direct synthesis of pressure sensitive adhesives from depolymerized raw lignocellulosic biomass. ACS Cent Sci 4(6):701–708. https://doi.org/10.1021/acscentsci.8b00140
39. Wörmeyer K, Ingram T, Saake B, Brunner G, Smirnova I (2011) Comparison of different pretreatment methods for lignocellulosic materials. Part II: influence of pretreatment on the properties of rye straw lignin. Bioresour Technol 102(5):4157–4164. https://doi.org/10.1016/j.biortech.2010.11.063
40. Yang W, Owczarek J, Fortunati E, Kozanecki M, Mazzaglia A, Balestra G et al (2016) Antioxidant and antibacterial lignin nanoparticles in polyvinyl alcohol/chitosan films for active packaging. Ind Crop Prod 94:800–811
41. Zhao M, Jing J, Zhu Y, Yang X, Wang X, Wang Z (2016) Preparation and performance of lignin–phenol–formaldehyde adhesives. Int J Adhes Adhes 64:163–167. https://doi.org/10.1016/j.ijadhadh.2015.10.010
42. Zhuang X, Wang W, Yu Q, Qi W, Wang Q, Tan X et al (2016) Liquid hot water pretreatment of lignocellulosic biomass for bioethanol production accompanying with high valuable products. 199:68–75

Publisher's note Springer Nature remains neutral with regard to jurisdictional claims in published maps and institutional affiliations.